



Deposited via The University of York.

White Rose Research Online URL for this paper:

<https://eprints.whiterose.ac.uk/id/eprint/91020/>

Version: Accepted Version

Article:

Taylor, Tiffany B., Mulley, Geraldine, Dills, Alexander H. et al. (2015) Evolutionary resurrection of flagellar motility via rewiring of the nitrogen regulation system. *Science*. pp. 1014-1017. ISSN: 0036-8075

<https://doi.org/10.1126/science.1259145>

Reuse

Items deposited in White Rose Research Online are protected by copyright, with all rights reserved unless indicated otherwise. They may be downloaded and/or printed for private study, or other acts as permitted by national copyright laws. The publisher or other rights holders may allow further reproduction and re-use of the full text version. This is indicated by the licence information on the White Rose Research Online record for the item.

Takedown

If you consider content in White Rose Research Online to be in breach of UK law, please notify us by emailing eprints@whiterose.ac.uk including the URL of the record and the reason for the withdrawal request.

**Title: Evolutionary resurrection of flagellar motility via rewiring of the
nitrogen regulation system**

Authors: Tiffany B. Taylor^{1†}, Geraldine Mulley^{1†}, Alexander H. Dills², Abdullah S. Alsohim^{1,3}, Liam J. McGuffin¹, David J. Studholme⁴, Mark W. Silby², Michael A. Brockhurst⁵, Louise J. Johnson^{1,*}, Robert W. Jackson^{1,6}

Affiliations:

¹School of Biological Sciences, University of Reading, Whiteknights, Reading, RG6 6AJ, UK

²Department of Biology, University of Massachusetts Dartmouth, 285 Old Westport Road, North Dartmouth, MA 02747, USA

³Department of Plant Production and Protection, Qassim University, Qassim, Saudi Arabia P.O. Box 6622

⁴College of Life and Environmental Sciences, University of Exeter, Stocker Road, Exeter, EX4 4QD, UK

⁵Department of Biology, University of York, Wentworth Way, York, YO10 5DD, UK

⁶The University of Akureyri, Borgir vid Nordurslod, IS-600 Akureyri, Iceland

*Corresponding author: L.J.Johnson@reading.ac.uk

† These authors contributed equally to this work

1 **One Sentence Summary:**

2 Rapid repeatable rewiring of regulatory networks: a nitrogen regulatory gene evolves a
3 new function, restoring flagella to immotile bacteria.

4

5 **Abstract:**

6 A central process in evolution is the recruitment of genes to regulatory networks. We
7 engineered immotile strains of the bacterium *Pseudomonas fluorescens* that lack
8 flagella due to deletion of the regulatory gene *fleQ*. Under strong selection for motility,
9 these bacteria consistently regained flagella within 96 hours via a two-step evolutionary
10 pathway. Step 1 mutations increase intracellular levels of phosphorylated NtrC, a distant
11 homologue of FleQ, which begins to commandeer control of the *fleQ* regulon at the cost
12 of disrupting nitrogen uptake and assimilation. Step 2 is a switch-of-function mutation
13 that redirects NtrC away from nitrogen uptake and towards its novel function as a
14 flagellar regulator. Our results demonstrate that natural selection can rapidly rewire
15 regulatory networks in very few, repeatable mutational steps.

16

17 **Main Text:**

18 A longstanding evolutionary question concerns how the duplication and
19 recruitment of genes to regulatory networks facilitates their expansion (1), and how
20 networks gain mutational robustness and evolvability (2). Bacteria respond to diverse
21 environments using a vast range of specialised regulatory pathways, predominantly
22 two-component systems (3), which are the result of adaptive radiations within gene

23 families. Due to past cycles of gene duplication, divergence and horizontal genetic
24 transfer, there is often extensive homology between the components of different
25 pathways (4), raising the possibility of cross-talk or redundancy between pathways (5).
26 Here we monitor the recovery of microbial populations from a catastrophic gene
27 deletion: bacteria engineered to lack a particular function are exposed to environments
28 that impose strong selection to re-evolve it, sometimes by recruitment of new genes to
29 regulatory networks (6, 7, 8, 9).

30 In the plant-associated soil bacterium *P. fluorescens*, the master regulator of
31 flagellar synthesis is FleQ (also called AdnA), a σ^{54} -dependent enhancer binding protein
32 (EBP) that activates transcription of genes required for flagellum biosynthesis (10, 11).
33 The starting *P. fluorescens* strain is AR2; this strain lacks flagella, due to deletion of
34 *fleQ*, and is unable to move by spreading motility due to mutation of viscosin synthase
35 (*viscB*), resulting in a distinctive, point-like colony morphology on spreading motility
36 medium (SMM) (12) (Figure 1A). We grew replicate populations of AR2 on SMM; when
37 local nutrients became depleted, starvation imposed strong selection to re-evolve
38 motility. To demonstrate that this finding was not strain-specific, these experiments were
39 replicated in a different strain of *P. fluorescens*, Pf0-2x. This strain is a $\Delta fleQ$ variant of
40 Pf0-1, already viscosin-deficient, and is thus unable to move by spreading or swimming
41 motility.

42 After 96 hours incubation of AR2 and Pf0-2x at room temperature on SMM, two
43 breakout mutations were visible conferring first slow (AR2S and Pf0-2xS) and then fast
44 (AR2F and Pf0-2xF) spreading over the agar surface (Fig. 1A). The AR2F strain
45 produces flagella, but we could not detect flagella in EM samples for AR2S (Fig. 1B).

46 Genome resequencing revealed a single nucleotide point mutation in *ntrB* in strain
47 AR2S, causing an amino acid substitution within the PAS domain of the histidine kinase
48 (HK) sensor NtrB (T97P). The fast-spreading strain AR2F had acquired an additional
49 point mutation in the σ^{54} -dependent EBP gene *ntrC*, which alters an amino acid
50 (R442C) within the DNA-binding domain (Table 1 & S2).

51 NtrB and NtrC comprise a two-component system: under nitrogen limitation NtrB
52 phosphorylates NtrC, which activates transcription of genes required for nitrogen uptake
53 and metabolism. To determine how mutations in this separate regulatory pathway
54 restored motility in the absence of FleQ, we performed microarray and qRT-PCR
55 analyses of the ancestral and evolved strains (Fig. S1 & Table S1). The expression of
56 genes required for flagellum biosynthesis and chemotaxis was abolished in AR2
57 compared to wild-type SBW25 (Fig. 2A). The *ntrB* mutation in AR2S partially restores
58 the expression of flagellar genes, and over-activates the expression of genes involved
59 in nitrogen regulation, uptake and metabolism. The subsequent *ntrC* mutation in AR2F
60 reduces the expression of nitrogen uptake and metabolism genes, while further up-
61 regulating flagellar and chemotaxis gene expression to wild-type levels (Fig. 2B). While
62 AR2S and AR2F showed higher growth rates than the ancestor in LB medium (the
63 medium on which the mutants arose; Tukey-Kramer HSD test, growth in LB compared
64 to AR2: AR2S, $P < 0.001$; AR2F, $P < 0.001$) (Fig. 1C), both mutants grew poorly in
65 minimal medium with ammonium as the sole nitrogen source (Tukey-Kramer HSD test,
66 growth in M9 + ammonium compared to AR2: AR2S, $P < 0.001$; AR2F, $P = 0.001$). This
67 is likely to be the result of ammonium toxicity due to the strong up-regulation of genes

68 involved in ammonium uptake and assimilation, indicating a pleiotropic cost of this
69 adaptation.

70 Sequencing of the *ntrBC* locus from independently evolved replicate strains
71 showed that evolution often followed parallel trajectories in both AR2 and Pf0-2x:
72 mutation of *ntrB* gave a slow-spreading strain and this was followed by mutation of *ntrC*
73 yielding a fast-spreading strain (Table 1; Fig. 3A & C). While all Pf0-2xF replicates
74 carried mutations in *ntrC*, several Pf0-2xS strains were not mutated in *ntrB*, suggesting
75 an alternative evolutionary pathway. Genome resequencing of these strains revealed
76 mutations in *glnA* or *glnK* (Table 1; Fig. 3B) likely to result in loss of function leading to
77 abnormally high levels of phosphorylated NtrC: reduced ammonium assimilation by
78 glutamine synthetase (*glnA*) would impose severe nitrogen limitation in the cell
79 irrespective of nitrogen availability, whereas GlnK is a PII-protein that regulates both
80 NtrB and glutamine synthetase activities.

81 These data suggest a predictable two-step evolutionary process: **Step 1**
82 increases levels of phosphorylated NtrC, via either (a) a direct regulatory route with
83 mutations in NtrB or GlnK, or (b) a physiological route with loss-of-function mutations
84 reducing glutamine synthetase activity and causing NtrB activation, partially or
85 intermittently reactivating the flagellar cascade. In **Step 2**, NtrC adapts to enhance
86 activation of the flagellar genes and in doing so, becomes a less potent activator of
87 nitrogen uptake genes. This model explains the microarray data and is consistent with
88 the predicted structural effects of the mutations (Figs. 2 and 3). Specifically, for NtrB the
89 structural changes are likely to either increase kinase or reduce phosphatase activity. In

90 support of this, the mutated NtrB(D228A) repeatedly emerging in Pf0-2xS resembles
91 NtrB(D227A) in *P. aeruginosa* which constitutively activates the Ntr system (13).

92 NtrC is a distant homologue of FleQ, sharing 30% amino acid identity and the
93 same three structural domains (TM-score > 0.7; $P < 0.001$; Fig. 3D) (14): an N-terminal
94 receiver domain, a conserved central σ^{54} -interacting domain, and a C-terminal DNA-
95 binding domain containing a helix-turn-helix (HTH) motif flanked by highly disordered
96 regions. We posit that an overabundance of phosphorylated NtrC activates transcription
97 of flagellar genes through functional promiscuity (15). Consistent with this, the *ntrC*
98 mutations in fast-spreading strains are predominantly located within or adjacent to the
99 HTH domain and likely influence enhancer-binding specificity; one is a frameshift
100 abolishing the HTH altogether (Fig. 3C). The evolved NtrC' must be constitutively
101 phosphorylated by overactive NtrB to enable its new multipurpose role, with the result
102 that flagellum biosynthesis and nitrogen regulation are probably no longer responsive to
103 environmental stimuli. Consequently, there is a trade-off between nitrogen utilization
104 and motility (Fig. 1A & C).

105 The flagellar regulatory network may have an unusually dynamic evolutionary
106 history. Flagella are expensive to make, and not always advantageous. Pathogens
107 expressing flagella can trigger strong immune responses in the host, so rapid transitions
108 are seen over short timescales between unflagellate, multiflagellate and aflagellate
109 states (16). This volatility is reflected in the structure of regulatory networks: in close
110 relatives of *Pseudomonas*, *fleQ* appears not to be involved in flagellar gene expression
111 (17), and in *Helicobacter pylori*, a gene of unknown function can be used as a “spare
112 part” to permit motility in *flhB* mutants (18). Our results illustrate that trans-acting

113 mutations can contribute to gene network evolution (19), but that as predicted, such
114 mutations bear severe pleiotropic costs (20, 21). Genes can retain the potential to take
115 on the functions of long-diverged homologues, suggesting that some degree of
116 evolutionary resilience is a consequence of regulatory pathways that evolve via gene
117 duplication. While *de novo* origination of new functions in nature is likely to take longer
118 and involve more mutational steps, this system enables us to understand the adaptive
119 process in detail at the genetic and phenotypic level. Here we identified a novel,
120 tractable model for gene network evolution and observed, in real time, the rewiring of
121 gene networks to enable the incorporation of a modified component (NtrC') creating a
122 novel regulatory function, by a highly repeatable two-step evolutionary pathway with the
123 same point mutations often recurring in independent lineages.

124

125 **References:**

- 126 1. J. R. True, S. B. Carroll, Gene co-option in physiological and morphological
127 evolution. *Annu. Rev. Cell. Dev. Bi.* **18**, 53-80 (2002).
- 128 2. M. Aldana, E. Balleza, S. Kauffman, O. Resendiz, Robustness and evolvability in
129 genetic regulatory networks. *J. Theor. Biol.* **245**, 433-448 (2007).
- 130 3. J. A. Hoch, Two-component and phosphorelay signal transduction. *Curr. Opin.*
131 *Microbiol.* **3**, 165-170 (2000).
- 132 4. S. A. Teichmann, M. M. Babu, Gene regulatory network growth by duplication.
133 *Nat. Genet.* **36**, 492-496 (2004).

- 134 5. E. J. Capra, M. T. Laub, Evolution of two-component signal transduction
135 systems. *Annu. Rev. Microbiol.* **66**, 325-347 (2012).
- 136 6. Z. D. Blount, C. Z. Borland, R. E. Lenski, Historical contingency and the evolution
137 of a key innovation in an experimental population of *Escherichia coli*. *Proc. Natl.*
138 *Acad. Sci. USA* **105**, 7899-7906 (2008).
- 139 7. J. R. Meyer, *et al.*, Repeatability and contingency in the evolution of a key
140 innovation in phage lambda. *Science* **335**, 428-432 (2012).
- 141 8. B. Hall, The EBG system of *E. coli*: Origin and evolution of a novel β -
142 galactosidase for the metabolism of lactose. *Genetica* **118**, 143-156 (2003).
- 143 9. D. Blank, L. Wolf, M. Ackermann, O. K. Silander, The predictability of molecular
144 evolution during functional innovation. *Proc. Natl. Acad. Sci. USA* **111**, 3044-
145 3049 (2014).
- 146 10. E. A. Robleto, I. López-Hernández, M. W. Silby, S. B. Levy, Genetic analysis of
147 the AdnA regulon in *Pseudomonas fluorescens*: Nonessential role of flagella in
148 adhesion to sand and biofilm formation. *J. Bacteriol.* **185**, 453-460 (2003).
- 149 11. N. Dasgupta, *et al.*, A four-tiered transcriptional regulatory circuit controls
150 flagellar biogenesis in *Pseudomonas aeruginosa*. *Mol. Microbiol.* **50**, 809-824
151 (2003).
- 152 12. A. S. Alsohim, *et al.*, The biosurfactant viscosin produced by *Pseudomonas*
153 *fluorescens* SBW25 aids spreading motility and plant growth promotion. *Environ.*
154 *Microbiol.* **16**, 2267-2281 (2014).

- 155 13. W. Li, C.-D. Lu, Regulation of carbon and nitrogen utilization by CbrAB and
156 NtrBC two-component systems in *Pseudomonas aeruginosa*. *J. Bacteriol.* **189**,
157 5413-5420 (2007).
- 158 14. D. J. Studholme, R. Dixon, Domain architectures of σ^{54} -dependent transcriptional
159 activators. *J. Bacteriol.* **185**, 1757-1767 (2003).
- 160 15. R. Wasseem, E. M. de Souza, M. G. Yates, F. D. Pedrosam, M. Buck, Two roles
161 for integration host factor at an enhancer-dependent *nifA* promoter, *Mol.*
162 *Microbiol.* **35**, 756-764 (2000).
- 163 16. E. Amiel, R. R. Lovewell, G. A. O'Toole, D. A. Hogan, B. Berwin, *Pseudomonas*
164 *aeruginosa* evasion of phagocytosis is mediated by loss of swimming motility and
165 is independent of flagellum expression. *Infect. Immun.* **78**, 2937-2945 (2010).
- 166 17. R. León, G. Espín, *flhDC*, but not *fleQ*, regulates flagella biogenesis in
167 *Azotobacter vinelandii*, and is under AlgU and CydR negative control.
168 *Microbiology* **154**, 1719-1728 (2008).
- 169 18. M. E. Wand, *et al.*, *Helicobacter pylori* FlhB function: The FlhB c-terminal
170 homologue HP1575 acts as a "spare part" to permit flagellar export when the
171 HP0770 FlhBCC domain is deleted. *J. Bacteriol.* **188**, 7531-7541 (2006).
- 172 19. H. E. Hoekstra, J. A. Coyne, The locus of evolution: evo devo and the genetics of
173 adaptation. *Evolution* **61**, 995-1016 (2007).
- 174 20. G. A. Wray, The evolutionary significance of *cis*-regulatory mutations. *Nat. Rev.*
175 *Genet.* **8**, 206-216 (2007).

- 176 21. S. B. Carroll, Evo-devo and an expanding evolutionary synthesis: a genetic
177 theory of morphological evolution. *Cell* **134**, 25-36 (2008).
- 178 22. M. W. Silby, *et al.*, Genomic and genetic analyses of diversity and plant
179 interactions of *Pseudomonas fluorescens*. *Genome Biol.* **10**, R51 (2009).
- 180 23. F. Van Immerseel, *et al.*, *Salmonella Gallinarum* field isolates from laying hens
181 are related to the vaccine strain SG9R. *Vaccine* **31**, 4940-4945 (2013).
- 182 24. K. Rutherford, *et al.*, Artemis: sequence visualization and annotation.
183 *Bioinformatics* **16**, 944-945 (2000).
- 184 25. D. B. Roche, M. T. Buenavista, S. J. Tetchner, L. J. McGuffin, The IntFOLD
185 server: an integrated web resource for protein fold recognition, 3D model quality
186 assessment, intrinsic disorder prediction, domain prediction and ligand binding
187 site prediction. *Nucleic Acids Res.* **39**, W171-W176 (2011).
- 188 26. L. J. McGuffin, M. T. Buenavista, D. B. Roche, The ModFOLD4 server for the
189 quality assessment of 3D protein models. *Nucleic Acids Res.* **41**, W368-W372
190 (2013).
- 191 27. L. J. McGuffin, Intrinsic disorder prediction from the analysis of multiple protein
192 fold recognition models. *Bioinformatics* **24**, 1798-1804 (2008).
- 193 28. D. B. Roche, M. T. Buenavista, L. J. McGuffin, The FunFOLD2 server for the
194 prediction of protein–ligand interactions. *Nucleic Acids Res.* **41**, W303-W307
195 (2013).
- 196 29. Y. Zhang, J. Skolnick, TM-align: a protein structure alignment algorithm based on
197 the TM-score. *Nucleic Acids Res.* **33**, 2302-2309 (2005).

Acknowledgments:

TBT, LJJ, RWJ and MAB conceived and designed the study. TBT, GM and AA performed experiments. MWS and AHD performed independent lines of enquiry on Pf0-2x. DS conducted bioinformatics analysis of genome resequencing data, identified mutated genes and handled sequencing data. LM conducted the protein structure prediction and analysis. This work was supported by a Leverhulme grant to LJJ, MAB and RWJ, BBSRC grant BB/J015350/1 to RWJ, start-up funding from the University of York to MAB, Qassim University to AA, and Agriculture and Food Research Initiative Competitive Grant 2010-65110-20392 from the USDA's National Institute of Food and Agriculture, Microbial Functional Genomics Program to MWS. TBT, GM, LJJ, RWJ, MWS, DJS and MAB wrote the paper. We thank Graham Bell, Mark Pagel, Angus Buckling and James Moir for useful discussions; Peter Ashton for processing of microarray data; and Konrad Paszkiewicz and Exeter Sequencing Service facility and support from the following: Wellcome Trust Institutional Strategic Support Fund (WT097835MF), Wellcome Trust Multi User Equipment Award (WT101650MA) and BBSRC LOLA award (BB/K003240/1). Sequence data for genomic resequencing of AR2S and AR2F have been submitted to the SRA under accession numbers SRR1510202 and SRR1510203, respectively. The eArray design ID for the microarray is 045642. Microarray data have been submitted to the ArrayExpress database under accession number E-MTAB-2788 (www.ebi.ac.uk/arrayexpress).

Figures 1 – 3:

Fig. 1. Phenotypic assays of motility variants.

A Surface spreading motility assays of ancestral (AR2) and evolved slow spreading (AR2S) and fast spreading (AR2F) mutants, after 27 hours. **B** Electron microscopy confirms the presence of a flagellum in AR2F, but fails to confirm presence in AR2S. **C** Mean (N=4) cell doublings per hour (+/- 1 SEM). Strains were grown in differing nitrogen environments: 10 mM glutamine (Gln), glutamate (Glu) and ammonium (NH₄) as the sole nitrogen source, or in high nutrient lysogeny broth (LB): AR2, $F_{3,12} = 13.460$, $P < 0.001$; AR2S, $F_{3,12} = 72.674$, $P < 0.001$; AR2F, $F_{3,12} = 52.538$, $P < 0.001$. There were also differences between doubling rate of strains within each nitrogen medium (Glutamate (Glu), $F_{2,9} = 12.654$, $P = 0.002$; Ammonium (NH₄), $F_{2,9} = 40.529$, $P < 0.001$), with the exception of Glutamine (Gln) ($F_{2,9} = 3.703$, $P = 0.067$).

Fig. 2. Heat map of microarray expression profiles for all evolved and ancestral motility variants.

Heat maps show where there is significant ($P \leq 0.05$) fold-change of ≥ 2 in genes selected based on GO-terms for **A** Bacterial-type flagellum (24 genes) and **B** Nitrogen compound transport (146 genes) for all strains. The gradation of colors reflects normalized raw signal values across the entire array. Genes are ordered according to chromosomal position to enable clearer visualization of coregulated gene clusters. Full transcriptome analysis is reported in Supplementary File “Microarray dataset.xlsx”.

Fig. 3. Full chain multi-template 3D models of protein structures of slow and fast spreading motility variants.

Slow spreading variants can either follow the direct regulatory route through mutation of NtrB or GlnK (**A**), or the physiological route through mutation of GlnA causing over-activation of NtrB (**B**); both routes are predicted to lead to hyperphosphorylation of NtrC. Fast spreading variants all show mutational changes to NtrC (**C**), which has a similar global structure to FleQ (**D**). The colour scheme represents the variation in models,

which correlates with local (per-residue) quality and disorder. Regions coloured in blue and green represent low local variability in structure, while those in red show high local variability (see Table 1 and Table S2 for mutation details). § = All mutations mapped onto SBW25 wildtype protein structures for illustrative purposes; * = Truncated domain.

	Slow Spreaders (AR2/Pf0-2xS) Hyperphosphorylation of NtrC	Fast Spreaders (AR2/Pf0-2xF) Switch of NtrC-P specificity
AR2	<i>ntrB</i> T97P*	<i>ntrC</i> R442C*
	<i>ntrB</i> V185K	<i>ntrC</i> K342E
	<i>ntrB</i> D179N	<i>ntrC</i> G452R
	<i>ntrB</i> L184Q / V185I	<i>ntrC</i> K342V / Frameshift: V342
Pf0-2x	<i>ntrB</i> D228A [§]	<i>ntrC</i> N454S
		<i>ntrC</i> R441S
		<i>ntrC</i> N454S
		<i>ntrC</i> P424L
		<i>ntrC</i> N454S
	<i>ntrB</i> D228A [§]	<i>ntrC</i> L418R
		<i>ntrC</i> G414D
		<i>ntrC</i> N454S
		<i>ntrC</i> F426V
	<i>glnK</i> Frameshift: I86*	<i>ntrC</i> R442H*
<i>glnA</i> T237P*	<i>ntrC</i> A445V*	
<i>glnA</i> Frameshift: T205*	<i>ntrC</i> R442C*	

* = Identified by genome resequencing

§ = Independent *ntrB* mutant strains, parent to multiple *ntrC* mutant strains

Table 1. Mutational trajectory towards slow and fast spreading phenotypes.

Mutations confirmed in slow spreading motility variants are predicted to result in hyperphosphorylation of NtrC; mutations in fast spreading variants lead to predicted switched specificity of NtrC-P towards FleQ targets. Slow and fast spreading variants share the same ancestry.

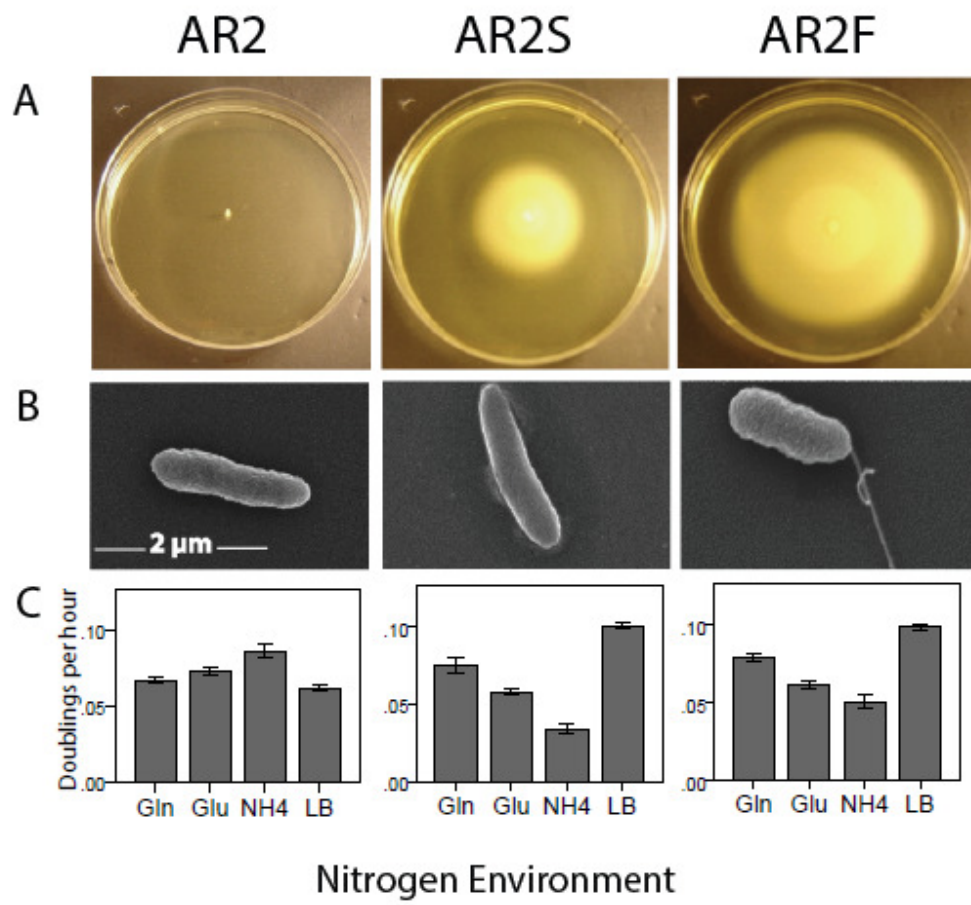


Figure 1

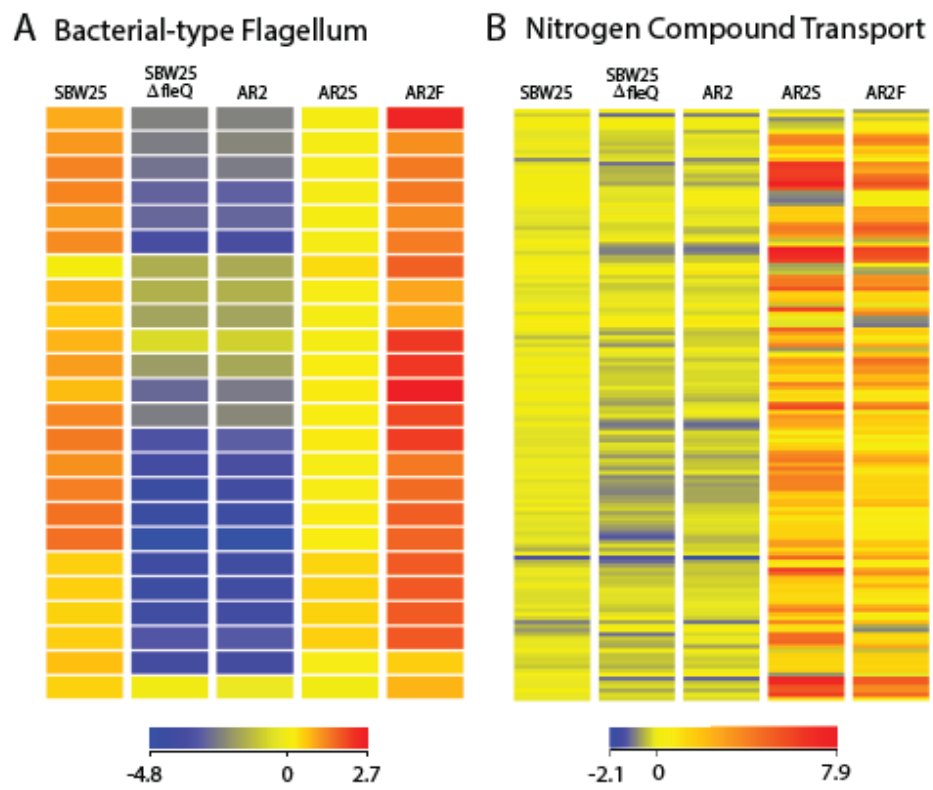


Figure 2

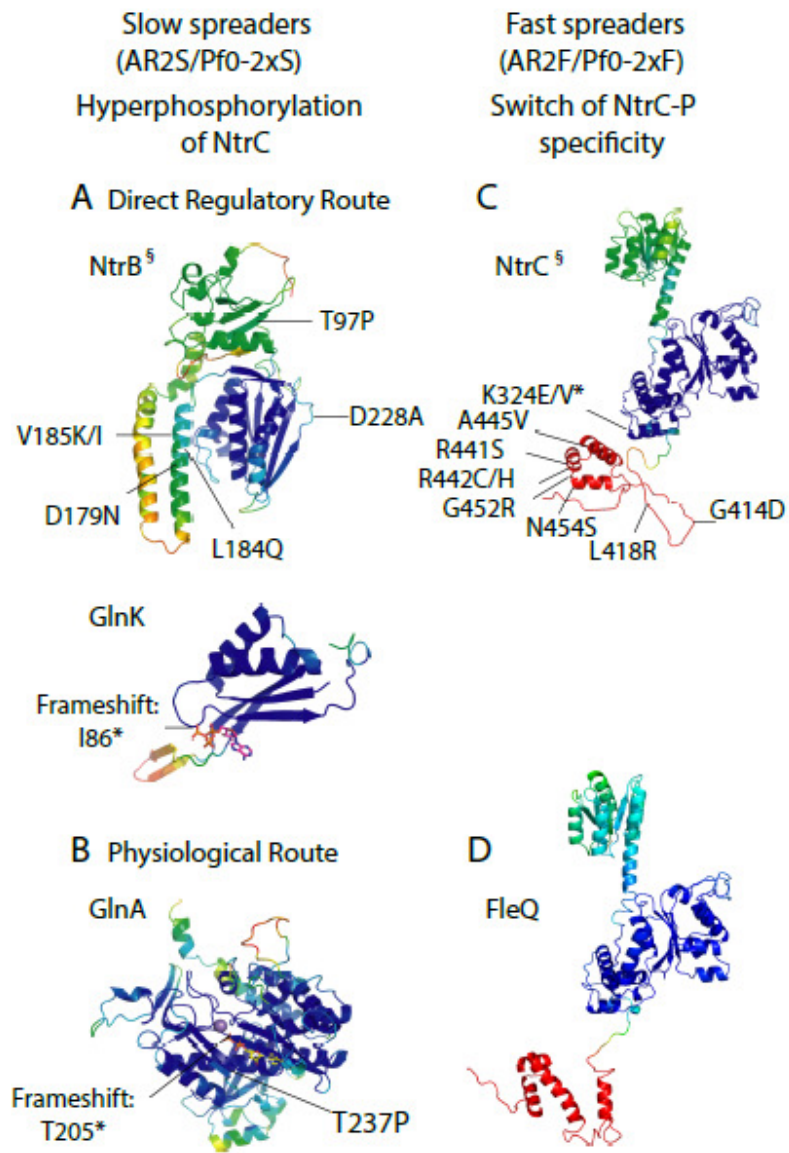


Figure 3

Supplementary Materials:

Title: Evolutionary resurrection of flagellar motility via rewiring of the nitrogen regulation system

Authors: Tiffany B. Taylor^{1†}, Geraldine Mulley^{1†}, Alexander H. Dills², Abdullah S. Alsohim^{1,3}, Liam J. McGuffin¹, David J. Studholme⁴, Mark W. Silby², Michael A. Brockhurst⁵, Louise J. Johnson^{1,*}, Robert W. Jackson^{1,6}

Materials and Methods

Fig. S1.

Table S1.

Table S2.

198 **Supplementary Materials:**

199

200 **Materials and Methods:**

201

202 **Microbiological methods**

203 *P. fluorescens* strains used in this study: SBW25, SBW25 Δ *fleQ*, AR2 (SBW25 Δ *fleQ* IS-
204 Ω Km-hah: PFLU2552), and Pf0-2x (Pf0-1 Δ *fleQ*). Motility assays are as described in
205 (12). All starting populations were from a single AR2 colony grown on LB agar (1.5%),

206 and stab inoculated into the center of a SMM plate using a sterile wire. The initial
207 observed motility mutants (AR2S and AR2F) were cultured immediately, cryopreserved
208 and used for subsequent genome resequencing and microarray analysis. Independently
209 evolved motility mutants were isolated from AR2 and Pf0-2x and cryopreserved.
210 Mutation rates of all lineages were checked by plating an overnight culture onto LB agar
211 supplemented with 100 $\mu\text{g ml}^{-1}$ rifampicin. All strains were found to have a similar
212 mutation frequency: SBW25 = 6.98×10^{-9} cfu ml^{-1} ; $\Delta\text{fleQSBW25}$ = 3.72×10^{-8} cfu ml^{-1} ;
213 AR2 = 2.50×10^{-8} cfu ml^{-1} ; AR2S = 2.3×10^{-8} cfu ml^{-1} ; AR2F = 1.4×10^{-8} cfu ml^{-1} .
214 M9 nitrogen modified medium (lacking ammonium) was supplemented with 10 mM
215 glutamate, glutamine or ammonium solutions. Strains were grown for 16 hours in LB at
216 27°C and diluted to OD 0.001 in M9 nitrogen modified media, and in LB. Optical density
217 595 nm was measured every 20 minutes, under continuous shaking and at an
218 incubation of 27°C, for 24 hours (Tecan, GENios).

219

220 **Molecular methods**

221 The mutations present in the original evolved mutants AR2S and AR2F, plus 3 Pf0-2xS
222 and 3 descended Pf0-2xF strains were identified by genome resequencing.

223 Genomic DNA was isolated using Puregene DNA extraction (Qiagen) or Wizard®
224 Genomic DNA Purification (Promega) kits. We resequenced the complete genomes of
225 mutants AR2S and AR2F (original) using the Illumina HiSeq and identified single-
226 nucleotide variants (SNV) by alignment to the SBW25 reference as described previously
227 (22, 23). Further mutants were analyzed by targeted PCR amplification and sequencing

228 of *ntrBC* to determine whether the same two-step process had occurred; primers were
229 designed to flank the region where SNVs had been identified by whole-genome
230 resequencing (NtrC, F: CTTTCATCCCCAACTCCTTGA, R:
231 AAGCTGCTGAAAAGCGAGAC; NtrB, F: CTTGCGCCTTGAGTACATGA, R:
232 ATGCGGTCTACCAGGTTACG).

233

234 *AR2S and AR2F Isolate Genome Resequencing Details*

235 Whole-genome resequencing was performed using the Illumina GA2x. We generated
236 12,065,035 pairs of 36-bp reads for AR2S (SRA accession SRR1510202) and
237 24,075,130 pairs of 36-bp reads for AR2F (SRR1510203). To identify mutations, we
238 aligned the genomic sequence reads against the *Pseudomonas fluorescens* SBW25
239 genome sequence (NCBI RefSeq accession NC_012660) using BWA-mem version
240 0.7.5a-r405 (<http://www.ncbi.nlm.nih.gov/pubmed/19451168>). We discarded reads that
241 did not uniquely map to a single location on the SBW25 genome in order to avoid
242 artifacts due to misalignment of sequence reads arising from repeat sequences. The
243 resulting average depths of coverage over the SBW25 genome were 124x and 144x for
244 AR2S and AR2F, respectively. For 99.86% of the SBW25 reference genome sequence
245 (6,713,197 out of 6,722,539 bp) we were able to unambiguously determine the
246 nucleotide sequence in both mutant genomes (on the basis that at these genomic
247 positions there was at least 95% consensus among all aligned reads at those positions
248 for each of the two resequenced genomes and depth of at least 5x). Over the 6,713,197
249 bp of the genome for which we could unambiguously determine the DNA sequence for
250 both mutant genomes, we found only three SNVs with respect to the reference genome

251 sequence. Two of these three variants were present in both resequenced genomes: at
252 position 376,439 both resequenced strains had a G whereas in the SBW25 reference
253 genome the base is T. This corresponds to a non-silent change from codon acc to
254 codon Ccc in gene PFLU0344 (*glnL/ntrB*). The second variant was at position 1,786,536
255 where SBW25 has A but the two resequenced mutants have G; this variant falls in an
256 intergenic region and we have no reason to suspect it has an effect on the phenotypes
257 observed. The third SNV is private to AR2F and falls within the gene PFLU0343
258 (*glnG/ntrC*). In SBW25 and AR2S the base is G but in AR2F it is A; this results in a non-
259 silent change from codon cgt to codon Tgt. Aside from these three variant sites, the
260 remainder of the 6,713,197 bp of unambiguously resolved genome sequence contained
261 no variation from the SBW25 reference genome.

262

263 *Pf0-2xS and Pf0-2xF Isolate Genome Resequencing Details*

264 Library preparation was performed using Illumina Nextera XT kit with Nextera XT
265 Indexes and sequenced as 250PE reads from MiSeq.

266 Whole-genome resequencing of Pf0-2x strains was performed using the Illumina MiSeq.
267 We generated 1,145,122 forward and 1,141,017 reverse reads of 251-bp for Pf0-2xS_1,
268 1,279,360 forward and 1,272,990 reverse reads of 251-bp for Pf0-2xF_1.1, 1,962,339
269 forward and 1,941,676 reverse reads of 251-bp for Pf0-2xS_2, 907,328 forward and
270 906,083 reverse reads of 251-bp for Pf0-2xF_2.1, 935,862 forward and 932,415 reverse
271 reads of 251-bp for Pf0-2xS_3, and 1,194,665 forward and 1,190,975 reverse reads of
272 251-bp for Pf0-2xF_3.1. These genomic sequence reads were mapped against the
273 *Pseudomonas fluorescens* Pf0-1 genome sequence (NCBI RefSeq accession

274 NC_007492.2) using CLC Genomics Workbench 6.0; unmapped reads were not
275 included in further analysis. The average coverage depths for each library were: 44.6 for
276 Pf0-2xS_1, 49.8 for Pf0-2xF_1.1, 76.1 for Pf0-2xS_2, 35.3 for Pf0-2xF_2.1, 36.4 for Pf0-
277 2xS_3, and 46.5 for Pf0-2xF_3.1. Out of the 6,438,405 bp Pf0-1 genome, 97.06-99.35%
278 of nucleotides (depending on sample) had a minimum 95% consensus among all
279 mapped reads. Using probabilistic variant detection to investigate unambiguous
280 nucleotide positions in each sequenced strain, we identified two SNVs and a 3bp
281 deletion common to all mutants (Table S2). These three common changes were also
282 present in the parental strain (Pf0-2x) and were thus not considered further. A 15bp
283 deletion was identified in both the Pf0-2xS1 and F1.1 strains with a unique SNV
284 occurring in the latter. An additional SNV was common to Pf0-2xS2 and Pf0-2xF2.1, yet
285 another to both Pf0-2xS3 and Pf0-2xF3.1, and a single unique SNV was discovered in
286 Pf0-2xF2.1 and another in Pf0-2xF3.1 with respect to the reference genome sequence.

287

288 The presence of *glnA*, *glnK* and *ntrC* mutations in resequenced strains was confirmed
289 by PCR of candidate regions from parental and evolved strains followed by Sanger
290 sequencing of the amplicons. Mutations in *ntrB* were detected by targeted PCR
291 amplification and sequencing, and *ntrC* mutations in derivatives of *ntrB* mutants were
292 detected the same way. In some cases, multiple primers were used to cover the full
293 length of the gene. This enabled us to be certain about the mutations, and rule out any
294 others. Primers used for Pf0-1 were: *ntrB*, F: ATTGCGCCTCGAGTACATGA and
295 TCGACACGGTTTCACTACGG, R: ATGCGGTGACACAGATTGCG and
296 TCGGAGCCTTGGTTTGGTTT; *ntrC*, F: AAGCTGCTGAAAAGCGAGAC and

297 GATTAAGGGTCACGGTGCCT, R: CTTCATGCCGAGTTCCTTGA and
298 CACTGGAACAAGGAGCCACA; glnA, F: GGAGGCCTTTCTTTGTCACG and
299 ACGCTTGTAGGAGTTGGTGG and CGGGAAGTAGCCACCTTTCA, R:
300 CCACCAACTCCTACAAGCGT and CAAGTCCGACATCTCCGGTT and
301 CTACCCGCCCTAATTCACCC; glnK, F: GCCGGGCATTACGATAGACA, R:
302 TGCCTTAGACTTGAGTCGG.

303

304 *Microarray design*

305 For microarray analysis, RNA was extracted from SBW25, SBW25 Δ *fleQ*, AR2, AR2S
306 and AR2F using an RNeasy kit (Qiagen) and assayed for quality [2100 Bioanalyzer
307 (Agilent), and Nanodrop 1000 Spectrophotometer (Thermo Fisher Scientific)]. RNA was
308 labelled, hybridised to custom Agilent arrays and scanned according to the
309 manufacturer's instructions (Technology Facility, Dept. of Biology, University of York,
310 UK). Differentially expressed genes were identified by ANOVA using the Benjamini-
311 Hochberg FDR correction. No commercially available microarrays were available for *P.*
312 *fluorescens*, so a custom design was created using the Agilent eArray system
313 (<http://earray.chem.agilent.com/earray>). The *P. fluorescens* SBW25 genome was
314 loaded into Artemis (24) (<http://www.sanger.ac.uk/resources/software/artemis>), and all
315 open reading frames marked as CDSs and these putative CDS written to a FASTA file
316 which was uploaded to eArray. A probeset was created containing five unique probes
317 per CDS, plus the appropriate Agilent control sequences. The probes were then laid out
318 onto a standard Agilent 8x60K format slide. Microarrays were validated using qRT-PCR
319 (MyiQTM, Bio-Rad).

320

321 *RNA labelling and hybridisation*

322 RNA isolated from each sample was labelled with Cy-3 using the Agilent Low Input
323 Quick Amp WT Labelling Kit (one color) according to the manufacturer's instructions.
324 Briefly, the RNA is reverse transcribed using a primer mix containing oligo-dT and
325 random nucleotide primers containing T7 promoters, then the cRNA amplified using the
326 T7 polymerase in the presence of Cy-3 labelled dCTP. The labelled cDNA was then
327 quality controlled and only samples with a specific activity of > 6 were used hybridised
328 to the arrays.

329 Samples were hybridised to the arrays, incubated and washed in accordance with the
330 manufacturer's instructions, and the slides scanned using an Agilent Microarray
331 Scanner and the fluorescence quantified with the Feature Extraction software. The
332 resulting files were then loaded into GeneSpring for further analysis.

333

334 *Initial Data Analysis*

335 GeneSpring software version 12.6 was used for all data analysis. Initial analysis was
336 performed to identify those genes that were differentially expressed between any
337 conditions in the experiment, followed by Gene Set Expression Analysis (GSEA) on the
338 basis of Gene Ontology terms. Briefly, the sample replicates were grouped, and then
339 ANOVA performed to identify differentially expressed genes, using the Benjamini-
340 Hochberg FDR p-value correction (with a FDR of 5%), and a Tukey HSD post-hoc test
341 used for each gene to identify which samples were significantly different from each

342 other for that gene. Those GO categories that were over-represented in the set of
343 differentially expressed genes were then identified.

344

345 **3D protein models**

346 The IntFOLD server (25) version 2 was used to build multi-template 3D models from the
347 wild type and mutant sequences of AdnA, NtrB, NtrC, FleQ, GlnA and GlnK. The 3D
348 models were quality checked using the ModFOLD4 protocol (26). Intrinsic protein
349 disorder was predicted using the DISOclust method (27). Binding sites were predicted
350 using the FunFOLD2 method (28). Models were structurally aligned and scored using
351 TM-align (29).

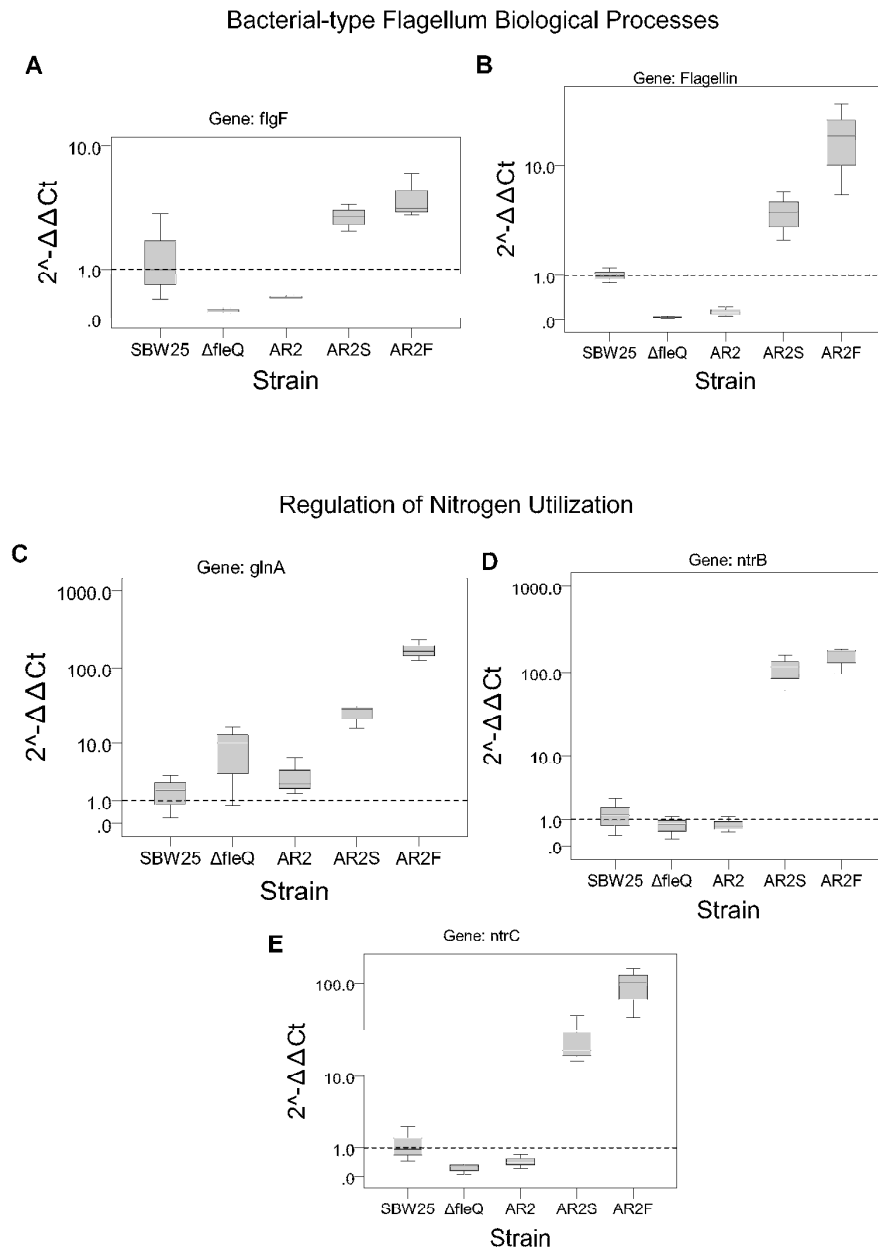
352

353 **Further Discussion of Microarray Results**

354 Full transcriptome analysis is reported separately in Supplementary File “Microarray
355 dataset.xlsx”. When genes were filtered for significant fold changes ($P \leq 0.05$) of ≥ 2 ,
356 and sorted by descending fold changes, the genes that showed the greatest changes in
357 expression are those highlighted in this study. Specifically, when comparing AR2 and
358 AR2S, the large majority of genes with greatest up regulation are related to nitrogen
359 transport, whereas when comparing AR2S to AR2F, the large majority of genes are
360 related to flagellar motility and chemotaxis.

361 Our microarray data show that the average level of flagella gene expression in AR2S is
362 between 1.5-2-fold lower than in SBW25, but considerably higher than AR2 (between 3
363 and 75 fold). There are at least two possible models to explain why we were unable to

364 observe flagella in AR2S: (i) Phosphorylated NtrC (NtrC-P) only weakly interacts with
365 flagella gene promoters, but the over-abundance of NtrC-P in AR2S saturates NtrC-
366 dependent promoters and the excess NtrC-P drives expression of flagella genes. The
367 level of transcription is suboptimal, thus the flagella may be unstable and support limited
368 or transient motility; (ii) Promiscuous activity of over-abundant NtrC-P (e.g. interacting
369 with RpoN from solution) leads to expression from flagella promoters, but this is not
370 equivalent in all cells and only a proportion of the population express sufficient levels to
371 produce a functional flagellum at any one time.



372

Fig. S1: Validation of gene expression changes detected by microarray using qRT-PCR.

A – E Box plots show gene expression, relative to wild-type SBW25, in genes related to nitrogen utilization and flagellar function. Note, data presented on log scales.

A. SBW25Δ*fleQ*

	GENE SYMBOL	GENE CHIP ARRAY		REAL TIME PCR	
		Fold Change	p-value	Fold Change	p-value
Bacterial-type Flagellum	<i>flgF</i>	-79.06	1.52E-07	-8.4	0.196
	Pflu4448 (Flagellin)	-158.33	2.09E-07	-22.59	0.002
Regulation of Nitrogen Utilization	<i>glnA</i>	1.01	2.24E-06	9.14	0.187
	<i>ntrB</i>	-1.54	1.37E-07	-4.5	0.41
	<i>ntrC</i>	-1.74	1.58E-07	-1.39	0.136

B. AR2

	GENE SYMBOL	GENE CHIP ARRAY		REAL TIME PCR	
		Fold Change	p-value	Fold Change	p-value
Bacterial-type Flagellum	<i>flgF</i>	-76.48	1.52E-07	-2.84	0.265
	Pflu4448 (Flagellin)	-128.22	2.09E-07	-6.61	0.004
Regulation of Nitrogen Utilization	<i>glnA</i>	1.03	2.24E-06	3.27	0.393
	<i>ntrB</i>	-1	1.37E-07	-2.24	0.424
	<i>ntrC</i>	-1.41	1.58E-07	-1.31	0.231

C. AR2S

	GENE SYMBOL	GENE CHIP ARRAY		REAL TIME PCR	
		Fold Change	p-value	Fold Change	p-value
Bacterial-type Flagellum	<i>flgF</i>	-2.53	1.52E-07	3.13	0.192
	Pflu4448 (Flagellin)	-1.71	2.09E-07	4.34	0.042
Regulation of Nitrogen Utilization	<i>glnA</i>	6.08	2.24E-06	25.49	0.008
	<i>ntrB</i>	28.18	1.37E-07	26.45	0.017
	<i>ntrC</i>	27.14	1.58E-07	49.14	0.059

D. AR2F

	GENE SYMBOL	GENE CHIP ARRAY		REAL TIME PCR	
		Fold Change	p-value	Fold Change	p-value
Bacterial-type Flagellum	<i>flgF</i>	1.1	1.52E-07	4.49	0.1
	Pflu4448 (Flagellin)	3.6	2.09E-07	16.57	0.065
Regulation of Nitrogen Utilization	<i>glnA</i>	11.34	2.24E-06	175.63	0.005
	<i>ntrB</i>	58.27	1.37E-07	96.09	0.006
	<i>ntrC</i>	63.72	1.58E-07	49.73	0.03

Table S1: Mean fold change (relative to SBW25) from qRT-PCR and microarrays with p-values (A – D).

Colours correspond to genes with significant (≥ 2 fold change) up regulated (red) and down regulated (blue) changes.

Strain	Nucleotide change	AA change	Gene	Domain/Function
AR2S_1	T376439G*	T97P	<i>ntrB</i>	PAS domain
AR2F_1.1	G374322A*	R442C	<i>ntrC</i>	HTH domain
AR2S_2	G376175A/ T376174A	V185K	<i>ntrB</i>	HK domain
AR2F_2.1	T374622C	K342E	<i>ntrC</i>	HTH domain
AR2S_3	G376193A	D179N	<i>ntrB</i>	HK domain
AR2F_3.1	C374291G	G452R	<i>ntrC</i>	Miscellaneous function
AR2S_4	G376176A T376174A	L184Q V185I	<i>ntrB</i>	HK domain
AR2F_4.1	T374622C/ /A374625	K342V FS from V342	<i>ntrC</i>	HTH domain
Pf0-2xS_1	Δ 6431771-3*	Δ G85	<i>gidB</i>	Methyltransferase domain
	Δ 6171472-87*	FS from I86	<i>glnK</i>	PII regulator
Pf0-2xF_1.1	C382879T*	R442H	<i>ntrC</i>	HTH domain
Pf0-2xS_2	Δ 6431771-3*	Δ G85	<i>gidB</i>	Methyltransferase domain
	T388861G* Δ 902225*	T237P FS from S544	<i>glnA</i> <i>carB</i>	Catalytic domain Miscellaneous function
Pf0-2xF_2.1	G382870A*	A445V	<i>ntrC</i>	HTH domain
Pf0-2xS_3	Δ 6431771-3*	Δ G85	<i>gidB</i>	Methyltransferase domain
	Δ 388958*	FS from T205	<i>glnA</i>	Catalytic domain
Pf0-2xF_3.1	G382880A*	R442C	<i>ntrC</i>	HTH domain
Pf0-2xS_4	A384603C	D228A	<i>ntrB</i>	Miscellaneous function
Pf0-2xF_4.1	A382843G	N454S	<i>ntrC</i>	HTH domain
Pf0-2xF_4.2	C382883A	R441S	<i>ntrC</i>	HTH domain
Pf0-2xF_4.3	A382843G	N454S	<i>ntrC</i>	HTH domain
Pf0-2xF_4.4	C382933T	P424L	<i>ntrC</i>	HTH domain
Pf0-2xF_4.5	A382843G	N454S	<i>ntrC</i>	HTH domain
Pf0-2xS_5	A384603C	D228A	<i>ntrB</i>	Miscellaneous function
Pf0-2xF_5.1	T382951G	L418R	<i>ntrC</i>	Miscellaneous function
Pf0-2xF_5.2	G382963A	G414D	<i>ntrC</i>	Miscellaneous function
Pf0-2xF_5.3	A382843G	N454S	<i>ntrC</i>	HTH domain
Pf0-2xF_5.4	T382928G	F426V	<i>ntrC</i>	HTH domain

* = Identified by genome resequencing.

Table S2: Full details of mutations identified in strains with parental AR2 and Pf0-2x origin.

Numbers before decimal points represent independent lineages, and numbers after represent derived strains. Note fast spreading mutants contain all nucleotide changes within a lineage.